EXPLORATION OF THE PHYSICAL PROPERTIES OF INTERNAL CHARACTERISTICS OF SUGAR MAPLE LOGS AND RELATIONSHIPS WITH CT IMAGES

Gerson Rojas Espinoza

Ph.D. Candidate
Centre de recherche sur le bois (CRB)
Département des sciences du bois et de la forêt
Université Laval
Québec/Québec G1K 7P4, Canada
and Assistant Professor
Departamento de Ing. En Maderas
Universitad del Bio-Rio, Casilla 5-C
Conception, Chile

Roger Hernández†

Centre de recherche sur le bois (CRB)
Département des sciences du bois et de la forêt

Alfonso Condal

Département des sciences géomatique
Université Laval
Québec/Québec, Canada G1K tP4

Daniel Verret

Forintek Canada Corp.
319 rue Franquet
Québec/Québec, Canada G1P 4R4

and

Robert Beauregard†

Centre de recherche sur les technologies de l'organisation réseau (CENTOR)
Centre de recherche sur le bois (CRB)
Département des sciences du bois et de la forêt
Université Laval
Québec/Québec, Canada G1K 7P4

ABSTRACT

Two groups of sugar maple (*Acer saccharum* Marsh) logs were scanned using an X-ray scanner to identify and locate their main internal characteristics. In the design of this exploratory study, five logs produced from a freshly cut tree (Group 1) and three logs (Group 2) sampled from a sawmill yard, were scanned to identify the various wood types present: rot; knots; colored heartwood; and sapwood. Based on these computed tomography (CT) images, four or five disks (20 mm thick) were cut from each log. Blocks of $10 \times 10 \times 10$ mm were then cut from each disk representing areas of each type of wood. The green density, basic density, and moisture content of each block were measured to assess within-tree

† Member of SWST.

variations between logs and within wood type. CT grey levels in the CT images were then measured for individual blocks to assess the feasibility of identifying wood types. Finally, a correlation analysis was carried out between physical properties and CT grey levels for each internal characteristic. The results generally indicated that, for both groups of logs, the type of wood was the most significant source of variation in green density, basic density, and moisture content. Statistically significant differences in these physical properties were also observed between sapwood and the other types of wood. This is a result of practical importance since sapwood in sugar maple is the main driver of product value. From the grey level variation observed in CT images, it is possible to separate sapwood from colored heartwood and knots. The contrast in grey level between the sapwood and the area of rot is not so obvious, but it can be enhanced by means of statistical methods. The correlation analysis indicated that green density was the variable that best correlated with grey level variations in CT images. A linear relationship between green density and grey level was established for each type of wood. The coefficient of determination (R^2) obtained from the simple regression analysis between grey level and green density varied between 0.32 and 0.82 depending on wood type. Nevertheless, significant differences were observed in the slopes of the curves. It is hypothesized that these differences could be mainly attributed to differences in the content and orientation of crystalline structures present in each type of wood.

Keywords: CT image, green density, moisture content, wood defects, sugar maple.

INTRODUCTION AND BACKGROUND

Sugar maple (*Acer saccharum* Marsh) is an important hardwood resource in Eastern Canada. This wood is mostly used in the production of furniture, flooring and cabinetry. In the hardwood sawmilling industry, the cost of raw material can represent up to 75% or more of total production costs (Steele et al. 1992). Thus, the optimization of value recovery from logs is a very critical factor. As each stage of the sawing process is destructive and irreversible, log shape and quality variability present a problem for sawmills.

Given that internal log defects in logs are unknown before sawing, the sawing process that turns logs into lumber has certain limitations. It is clear that knots, cracks, rot, and other anomalies determine final lumber value. Steele et al. (1994) indicated that the value of red oak lumber might be increased by 10% depending on the ability to locate internal defects in a log and to position it for the optimum cutting pattern. In the case of sugar maple, the presence of colored heartwood also reduces the final price that can be obtained for lumber. For example, the value of sapwood grade can be three times the value of regular grade wood.

The basic goal in sawing logs is to create boards with a maximum of clear faces. Operators have so far relied on external log appearance to predict the location of internal defects, but

emerging techniques are becoming available to reveal the internal morphology of sawlogs in a nondestructive way. These include ultrasounds (Birkeland and Han 1991), magnetic nuclear resonance (Chang et al. 1989), and X-ray. X-ray techniques, including computerized tomography (CT), have been the most widely investigated. Information on internal log defects by CT scanning has been obtained by Funt and Bryant (1987); Wagner et al. (1989); Zhu et al. (1991); Guddanti and Chang (1998); and Bhandarkar et al. (1999). Other studies have been conducted on the localization of knots (Taylor et al. 1984; Nordmark 2002), the prediction of the interior knot parameter (Björklund 1997; Björklund and Petersson 1999; Moberg 2000; Oja 2000), the classification of knots (Hagman and Grunbderg 1995), and the detection of resin pockets (Oja and Temnerud 1999). Almost nothing has ever been reported, however, on X-ray detection of internal defects (including colored heartwood) in sugar maple logs.

In a CT scanner, the X-ray source and a diametrically positioned detector array rotate synchronously around the object to be imaged. In one rotation, the X-ray beam travels through the object from several hundred directions, and the detectors provide corresponding transmission measurements. The transmission profile, which is a one-dimensional X-ray image, is called a projection. Each detector measures the signal in-

tensity (I) and, when the initial intensity (I_0) is known, the attenuation along the transmission path can be determined. The attenuation is a function of the local attenuation coefficient in the material:

$$I = I_0 e^{-\int \mu(x)dx} \tag{1}$$

where the integration variable x is the linear co-ordinate along the propagation path, e is Euler's constant (2.718), and $\mu(x)$ is the attenuation co-efficient as a function of the position. The at-tenuation coefficient reflects the degree to which X-ray intensity is attenuated by an object.

CT scanning produces images that lie in the same plane as the X-ray beam. By measuring many simultaneous ray-sums and continually ro-tating the source-detector pair, one can generate a detailed 2-D, cross-sectional image or tomo-graph, and a succession of 2-D images can serve to determine the internal appearance of a 3-D object. An image consists of a rectangular array of picture elements (pixels), where each pixel represents the attenuation coefficient of small volume elements (voxels). This voxel is deter-mined by the size of the image pixel and the thickness of the X-ray beam (Platten 2002). The grey level value of each picture element of a CT image is called CT number. The CT number represents the calculated attenuation of the vol-ume representing the CT voxel of X-ray trans-mission. The linear attenuation coefficient varies with the composition and density of the material (Seeram 2001).

The density of wood is an important param-eter because it is related to many anatomical and physical properties and, consequently, to wood quality. Knowledge of wood density generally makes it possible to differentiate characteristics present in logs, such as knots, bark, decay, sap-wood, heartwood, voids, etc. However, differen-tiation of these characteristics from CT scanner images also requires information on moisture content (MC). Unfortunately, data on variations in the green density (GD), basic density (BD), and moisture content of sugar maple logs are rather scarce. The literature offers only a few references on moisture content variations (Good

et al. 1955; Panshin and de Zeeuw, 1980), and basic density variations (Lamb and Marden 1968, 1970). The interpretation and analysis of results obtained from CT images are limited by the lack of information on density and moisture content variations between wood types. A better understanding of the physical characteristics variation associated with the different wood types and their relationships with CT image grey levels would consequently help using X-ray techniques to nondestructively identify and lo-cate internal defects in sugar maple logs, and guide sawing decisions.

The first objective of this exploratory study was to assess the level of variation in green den-sity, basic density, and moisture content between rot, knots, colored heartwood and sapwood found in sugar maple logs. The second objective was to measure the grey level of the specimens in CT images and determine the corresponding spectral range for each internal characteristic. The last objective was to establish relationships between CT grey levels and the physical prop-erties of the various types of wood in order to assess the ability of X-ray technology to identify and locate internal defects in sugar maple.

MATERIALS AND METHODS

Selection of materials and CT scanning

Two groups of sugar maple logs were used in this study. The logs were selected on the basis of external characteristics such as diameter, the presence of branches, and rot. The first group consisted of five six-foot-long logs collected at the beginning of August 2002 from one standing tree in the Duchesnay forest, 45 km North-East of Quebec City. Once the tree was felled, logs were crosscut and bark was left on. The second group consisted of three six-foot-long logs se-lected in a sawmill yard located in the Portneuf region of the Province of Quebec. The time and location of tree harvest were unknown. This sec-ond group of logs was debarked at a sawmill.

Both groups of logs were then scanned with a Siemens Somaton X-ray CT scanner at the Natu-ral Resource Scanography Laboratory owned

and operated jointly by the Institut National de la Recherche Scientique (INRS), Forintek Canada Corp., and Université Laval, in Quebec City. Scanning was performed at 140 Kvp and 119 mA with a slice plane of 5 millimetres in thickness. Each slice was saved as a 512×512 image with a radiometric resolution of 12 bits. One group of log images was then selected to study the presence of rot, knots, colored heartwood and sapwood. The CT images, initially in Digital Imaging and Communication in Medicine (DICOM) format, were transformed to bitmap (.bmp) format at 8 bits of resolution using the CT viewer software provided by Siemens. The mean pixel resolution used was 0.4×0.4 mm.

Specimen preparation

Specimens for the determination of green density, basic density, and moisture content were obtained from disks taken from the sample logs. To identify the actual longitudinal position of each CT image in a log (z axis), each log was marked, and 20-mm-thick disks were cut with a portable bandsaw at the rate of four or five disks per log. The disks were labelled and kept frozen in plastic bags to avoid drying. On each disk, two 10-mm-wide strips were traced perpendicularly from bark to bark passing through the pith. A digital photo of each transverse section of the disk was taken with a Kodak DX 3215 digital camera. The strips were then cut into 10-by-10-mm sections of variable lengths, depending on disk diameter. Each strip was crosscut at 10-mm increments with a 0.7-mm kerf bandsaw, producing blocks of $10 \times 10 \times 10$ mm. Photos were then used as references to identify the position of each block in the disk. The blocks were labelled and kept frozen in plastic bags. The number of blocks obtained from each disk varied from 42 to 61.

Density and moisture content determination

The green mass of each block was measured to the nearest 0.001g. Green volumes were determined by the water-displacement method. All blocks were then oven-dried at 103°C until a constant weight was reached (24 h). After cooling to room temperature, their oven-dry mass was measured to the nearest 0.001g. Green density was calculated as the green mass to green volume ratio. Basic density was calculated as the oven-dry mass to green volume ratio. Moisture content was expressed as a percentage of oven-dry mass. Following measurement, the blocks were sorted into groups according to the presence of rot, knots, colored heartwood and sapwood. The resulting data were analyzed by variance analysis with the SAS software. Contrast procedures were used to compare differences between means for all variables obtained for each type of wood within each group of logs.

Spatial analysis of CT images

A method to obtain the CT image grey level representing the volume of each block was developed. Initially, a group of five consecutive CT images representing the thickness of each disk was identified by reference to the digital photos of each disk. Next, polygons equivalent to the surface areas of the transverse cross-sections of the blocks were obtained. Finally, as the blocks were taken from the center of each disk, the value of the grey level corresponding to the volume of each block (polygon) was determined on the basis of only the three median consecutive CT images of each group. Nonetheless, the position of the log in a coordinate system (x, y) during the scanning process was different from its position during the marking, cutting, and photographing of the disk. As a result, CT images were not in the same orientation as the standard x, y orientation, which made it impossible to obtain grey level values representative of each block volume directly from images. In order to solve this problem, a pre-processing operation called geometric correction, was applied to each set of CT images.

The PCI Geometric Correction software (PCI 1997) was used to carry out image-to-image geometric corrections. The uncorrected image was referred as the CT image (Fig.1a), and the master image was the digital photo of the corresponding slice (Fig. 1b). The first step in the
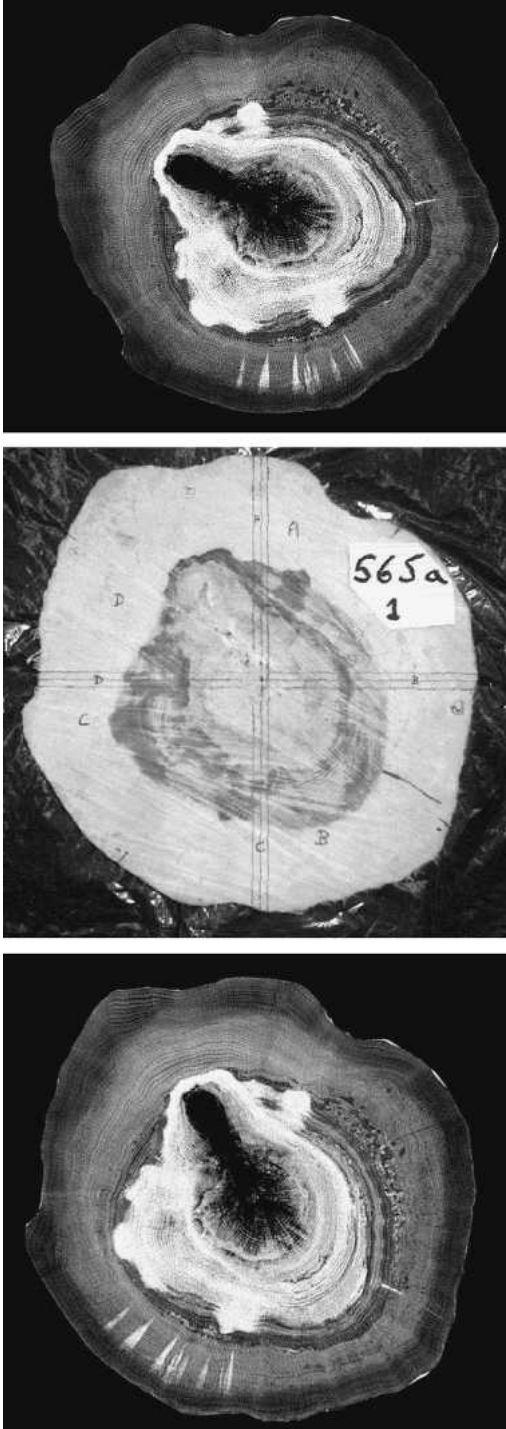
FIG. 1. Description of geometric correction steps. A. Uncorrected CT image B. Master image C. Corrected CT image.

geometric correction process was to warp the input into the master image. Next, the resampling process was performed to determine pixel value in the output image. This procedure was performed according to the method described by Jensen (1996). The number of control points and the order polynomial were selected to a root means square (RMS) error equal to or smaller than one pixel. Given that each group consisted of five images, a test was performed to assess the need for individual geometric corrections in the different groups. Uncorrected images 1, 3, and 5 were corrected twice, with the digital photo of one side of the disk as master in the first pass, and the digital photo of the other side in the second pass. As the RMS values obtained were identical, the polynomial obtained for the first CT image in each group was applied directly to the three other images of the group. In total, 45 geometric corrections were performed, using a second order polynomial, 15 control points and an RMS error of about one pixel.

Determination of grey level values for individual specimens

The PCI software is a raster system; it was found that a vector system (ESRI Arcview 3.1 software 1999) was more appropriate to deal with the representation of the polygons. With the digital photo as a reference, the center coordinates x, y of each disk were identified. Subsequently, the x, y coordinates of the four vertices of each specimen (polygon) were determined on the basis of the center coordinates, the block dimension, the saw kerf, and the resolution of the CT image. The grey level value of the corresponding section of each specimen (block polygon) was then obtained with the Arcview 3.1 software by superposition of the polygon coordinates over the corresponding CT image (Fig. 2). These values correspond to the mean value of the total number of pixels contained in the surface area of each block polygon represented in the CT image. The final grey level value, corresponding to the volume of each specimen, was determined as the mean value obtained from the set of three consecutive CT images contained in
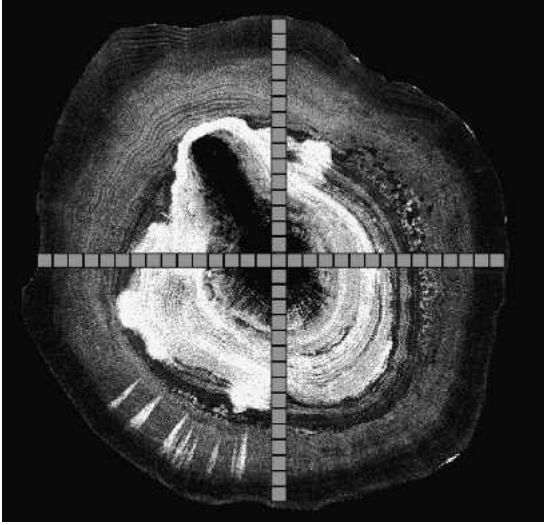
FIG. 2.   Grey level determination in specimen blocks using the Arcview 3.1 software.

the block thickness. With a mean resolution of 0.4 mm per pixel (25 pixels per 10 mm), the number of voxels contained in each block specimen was approximately 1875 ($25 \times 25 \times 3$ CT images).

RESULTS AND DISCUSSION

Physical properties

The mean green density, basic density, and moisture content values obtained for rot, knots, colored heartwood and sapwood in logs from a freshly cut tree (Group 1) and logs chosen at the sawmill yard (Group 2) are presented in Tables 1 and 2, respectively. For Group 1, only the first two logs had rot, which was located in the colored heartwood zone. For Group 2, only one log had rot, in the colored heartwood zone. In this group, logs 1 and 3 had colored heartwood and logs 1 and 2 had knots. The results of the analysis of variance and contrast for both groups of logs are shown in Table 3.

Moisture content

The moisture content results obtained for rot, knots, colored heartwood and sapwood from Groups 1 and 2 are presented in Tables 1 and 2, respectively. As indicated, the rot specimens ex-

hibited high moisture content values, with 141.3% and 103.1%, respectively for Group 1 and 2 logs. It was also observed that the mean moisture content values for colored heartwood and sapwood in Group 1 were about 82.6% and 60.1%, respectively. These differ from the corresponding 65% and 72% values reported by Simpson and TenWolde (1999). To a large extent, the difference can be attributed to the tree harvest seasonal variation between the two studies (Clark and Gibbs 1957). The mean moisture content value for knots was 78.5%.

The logs in Group 2 generally had lower mean moisture contents than those in Group 1. This can be attributed to the storage time (forest and sawmill yard) and to the absence of bark, both of which favored drying. In addition, the seasonal variation associated with harvesting time influenced the moisture content of the tree; in the case of Group 2 logs, the harvesting date was not known. The knots of the logs in this group exhibited a large moisture content variation, with maximum and minimum mean values of 71.3% and 40.9%, respectively. The colored heartwood had a maximum mean value of 80.7% and a minimum mean value of 54.3%. The minimum mean value observed for the sapwood was 36.9% and the maximum mean value was 47.6%. For the whole group, the mean moisture content values for knots, colored heartwood and sapwood (when these characteristics were present) were 56.1, 67.5, and 43.1%, respectively.

The analysis of variance showed that wood type was the most significant source of moisture content variation (Table 3). The differences in moisture content across log height in Group 1, the freshly felled tree, were nonsignificant while these were highly significant among the Group 2 logs, whose origins were less well defined. The differences in moisture content between sapwood–rot, sapwood–knots and sapwood–colored heartwood observed within Groups 1 and 2 were statistically highly significant.

Basic density

The sapwood and colored heartwood specimens from Group 1 showed mean basic density

TABLE 1. *Summary of green density, basic density, moisture content, and grey level values for rot, knots, colored heartwood and sapwood from a freshly harvested tree.*

Height level	Type of wood	n	Physical properties[1]			
			Green density (g/cm³)	Basic density (g/cm³)	Moisture content (%)	Grey level
1	Rot	32	0.877 (0.141)[2]	0.358 (0.088)	151.8 (39.9)	67 (46.9)
	Knot	15	1.158 (0.026)	0.660 (0.039)	75.8 (9.7)	227 (11.3)
	Heartwood	39	1.117 (0.034)	0.608 (0.029)	84.1 (8.5)	210 (19.2)
	Sapwood	105	0.924 (0.024)	0.584 (0.014)	58.1 (3.0)	95 (8.1)
2	Rot	13	0.885 (0.072)[2]	0.387 (0.053)	130.8 (21.5)	65 (31.2)
	Knot	9	1.163 (0.019)	0.632 (0.025)	84.2 (5.5)	221 (11.8)
	Heartwood	44	1.127 (0.033)	0.607 (0.029)	85.9 (7.9)	220 (20.4)
	Sapwood	100	0.925 (0.022)	0.585 (0.011)	58.3 (4.2)	103 (10.6)
3	Rot	n/a	n/a	n/a	n/a	n/a
	Knot	26	1.159 (0.040)	0.666 (0.050)	74.7 (11.7)	233 (13.7)
	Heartwood	78	1.071 (0.037)	0.589 (0.027)	82.0 (6.9)	191 (24.0)
	Sapwood	95	0.939 (0.020)	0.583 (0.010)	61.1 (3.8)	117 (11.1)
4	Rot	n/a	n/a	n/a	n/a	n/a
	Knot	23	1.158 (0.036)	0.666 (0.030)	74.0 (8.1)	234 (14.3)
	Heartwood	68	1.062 (0.048)	0.593 (0.034)	79.4 (7.6)	170 (29.9)
	Sapwood	96	0.972 (0.029)	0.595 (0.017)	63.4 (4.2)	116 (11.1)
5	Rot	n/a	n/a	n/a	n/a	n/a
	Knot	10	1.195 (0.023)	0.652 (0.043)	83.8 (9.5)	242 (11.5)
	Heartwood	54	1.118 (0.037)	0.615 (0.035)	81.7 (7.6)	193 (26.4)
	Sapwood	62	0.986 (0.022)	0.617 (0.019)	59.8 (4.8)	121 (15.3)

[1] Mean values
[2] Standard deviation in parentheses
n/a: not available.

TABLE 2. *Summary of green density, basic density, moisture content, and grey level values for rot, knots, colored heartwood and sapwood in logs from a sawmill yard.*

Log	Type of wood	n	Physical properties[1]			
			Green density (g/cm³)	Basic density (g/cm³)	Moisture content (%)	Grey level
1	Rot	20	0.854 (0.117)[2]	0.423 (0.066)	103.1 (15.1)	64 (45.5)
	Knot	5	1.164 (0.045)	0.686 (0.085)	71.3 (16.6)	239 (18.3)
	Heartwood	145	1.074 (0.037)	0.594 (0.030)	80.7 (8.7)	203 (22.7)
	Sapwood	121	0.895 (0.051)	0.606 (0.027)	47.6 (6.9)	89 (32.8)
2	Rot	n/a	n/a	n/a	n/a	n/a
	Knot	25	0.939 (0.042)	0.666 (0.022)	40.9 (3.2)	226 (15.7)
	Heartwood	n/a	n/a	n/a	n/a	n/a
	Sapwood	126	0.856 (0.026)	0.625 (0.018)	36.9 (1.1)	123 (22.2)
3	Rot	n/a	n/a	n/a	n/a	n/a
	Knot	n/a	n/a	n/a	n/a	n/a
	Heartwood	102	0.946 (0.099)	0.613 (0.041)	54.3 (10.6)	157 (55.4)
	Sapwood	195	0.859 (0.064)	0.592 (0.033)	44.9 (5.7)	110 (46.8)

[1] Mean values
[2] Standard deviation in parentheses
n/a: not available.

values of 0.595 and 0.602 g/cm³, respectively (Table 1), and no trend was detected with respect to height position. For Group 2, the results indicated mean basic density values of 0.604 and 0.607 g/cm³ for colored heartwood and sapwood, respectively (Table 2). Mean values of

TABLE 3. *Analysis of variance and contrast for physical properties for both log groups.*

Source of variation	df	Green density			Basic density			Moisture content		
		Mean square	F value	Pr > F	Mean square	F value	Pr > F	Mean square	F value	Pr > F
Group 1										
Height	4	0.0459	22.82	<.0001	0.0143	15.32	<.0001	35.1291	0.33	0.8607
Type of wood	3	2.0578	1022.79	<.0001	0.7911	847.18	<.0001	109081.8835	1012.00	<.0001
Contrast										
Sapwood-rot	1	0.1328	66.02	<.0001	1.8472	1977.95	<.0001	277193.9827	2571.62	<.0001
Sapwood-knots	1	3.3275	1653.91	<.0001	0.3394	363.44	<.0001	19180.7597	177.95	<.0001
Sapwood-heartwood	1	3.7296	1853.74	<.0001	0.0136	14.61	0.0001	85535.0664	793.54	<.0001
Heartwood-rot	1	1.4674	729.38	<.0001	1.8415	1971.81	<.0001	140643.1768	1304.80	<.0001
Heartwood-knots	1	0.3417	169.83	<.0001	0.2397	256.67	<.0001	1934.3656	17.95	<.0001
Knot-rot	1	2.0767	1032.19	<.0001	2.2727	2433.54	<.0001	127881.5857	1186.41	<.0001
Group 2										
Log	2	0.4600	109.70	<.0001	0.3208	28.92	<.0001	17058.9409	210.13	<.0001
Type of wood	3	0.9695	231.16	<.0001	0.2203	198.58	<.0001	28377.6821	349.55	<.0001
Contrast										
Sapwood-rot	1	0.0878	20.93	<.0001	0.5529	498.40	<.0001	42360.7752	521.79	<.0001
Sapwood-knots	1	0.3277	78.14	<.0001	0.0633	57.09	<.0001	1062.0088	13.08	0.0003
Sapwood-heartwood	1	2.2793	543.48	<.0001	0.0024	2.16	0.1424	58715.3973	723.24	<.0001
Heartwood-rot	1	0.7261	173.12	<.0001	0.5856	527.86	<.0001	13891.9043	171.12	<.0001
Heartwood-knots	1	0.0068	1.63	0.2025	0.0460	41.49	<.0001	4692.0768	57.80	<.0001
Knot-rot	1	0.3673	86.25	<.0001	0.5492	495.05	<.0001	19270.8144	237.37	<.0001

basic density for sapwood and colored heartwood were generally in agreement with those reported by Lamb and Marden (1968, 1970) for sugar maple wood. The knot specimens for Groups 1 and 2 showed denser wood, with mean basic density values of 0.656 and 0.676 g/cm^3, respectively. Rot specimens showed mean basic density values of 0.373 and 0.422 g/cm^3 for Groups 1 and 2, respectively (Tables 1 and 2). Rot leads to a decrease in basic density through the degradation of the solid wood components.

The variance analysis on basic density results indicated that, for both groups, wood type was the most significant source of variation. Within Group 1, differences in basic density between sapwood–rot, sapwood–colored heartwood, and sapwood–knots, were statistically significant. For Group 2, the same contrasts were significant except for the sapwood–colored heartwood, where they were not statistically significant.

Green density

Basic density and moisture content are fundamental in determining wood type physical prop-

erties. Nevertheless, given that a CT scanner measures the attenuation of an X-ray signal, it is expected that green density should be the physical property most closely related to CT image grey levels. For this reason, it was decided to study green density variability in sugar maple logs. For Group 1, the means of green density for rot, knots, colored heartwood and sapwood were 0.881, 1.167, 1.099, and 0.949 g/cm^3, respectively (Table 1). The green density values in sapwood specimens tended to increase with log height. This same trend was not observed for colored heartwood and knots. For Group 2, the means of green density for rot, knots, colored heartwood and sapwood were 0.854, 1.052, 1.010, and 0.870 g/cm^3 respectively. As expected, the variation in green density was the result from a combination of basic density and moisture content. For instance, lower moisture content values in sapwood than in colored heartwood resulted in lower green density values in sapwood than in colored heartwood.

The variance analysis indicated once again that, for both groups of logs, wood type was the

most significant source of variation in green density (Table 3). Also the contrast between sapwood and any of the other wood types (rot, knots, and colored heartwood) within Groups 1 and 2 was highly significant. This result is of practical importance since the value of lumber in sugar maple is driven by the presence of sapwood and the absence of the other wood types. The ability to separate the sapwood from other wood types on the basis of green density appears to be key in eventually being able to use X-ray for sawing optimization.

Analysis of CT images

Typical CT images obtained from Groups 1 and 2 are shown in Figs. 3a and 3b, respectively. These images clearly show internal log characteristics such as knots, colored heartwood, sapwood, bark (Fig. 3a), and rot (Fig. 3b). These characteristics appear as light or dark zones (respectively of high or low density) or as discontinuities in the normal growth ring pattern of the log. Knots can be easily identified in Fig. 3a by their whiteness (due to denser wood), their elliptical form, and the change in wood grain occurring in their vicinity. Colored heartwood generally appears in a circular shape and is located around the pith. Nonetheless, a variation in grey level across growth rings can be observed inside the colored heartwood area, and this can be attributed mostly to a moisture content variation. The area corresponding to sapwood has a darker color and is of greater homogeneity in grey level, with a clear distinction between growth rings, which contrasts with the other areas and should help identification.

Rot is identified by its dark color and by a rupture in the ring pattern (Fig. 3a). This defect was always observed within the colored heartwood area. A marked contrast could, however, be seen between these two types of wood. In log Group 2, sapwood generally appeared as having two regions: an inner region, of a slightly clearer shade, near the colored heartwood, and an outer region, which was darker. This can be explained mainly by the lower moisture content present in
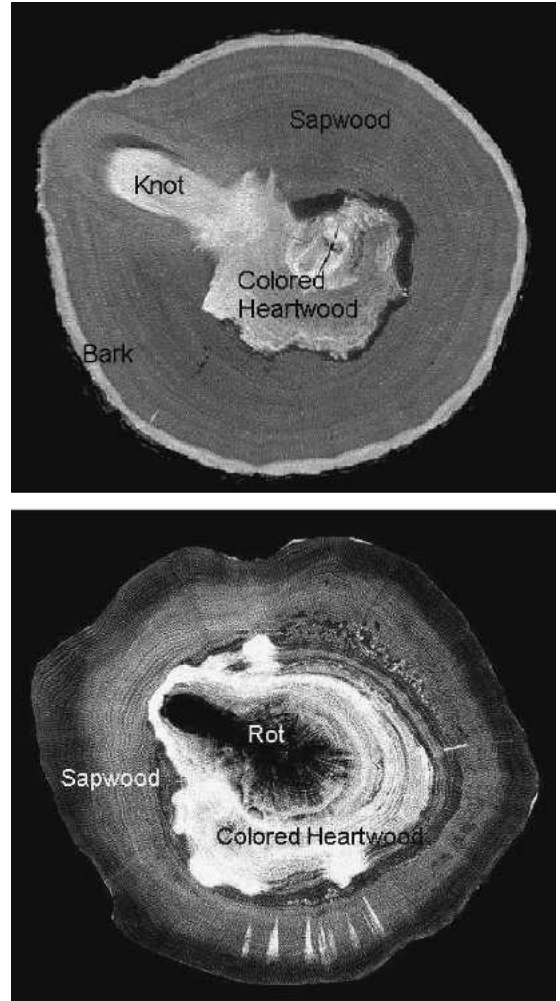

Fig. 3.   Sugar maple log CT images. (a) Group 1 showing the presence of bark and a knot. (b) Group 2 showing the presence of rot.

the outer area due to storage in the absence of bark.

The mean values of signatures (grey levels) obtained for all characteristics in both groups are presented in Tables 1 and 2. It was generally possible to distinguish sapwood from knots and colored heartwood in terms of grey level. However, there was a degree overlap between the signatures of sapwood and rot. This overlap can be explained by the combined effect of higher moisture content and lower basic density in the rot specimens, compared to lower moisture con-

tent and greater basic density in sapwood. Som et al. (1995) reported a similar situation for eucalyptus logs. They also indicated that severe rot was easily differentiated, but for incipient rot the precise boundaries of the infected area were more difficult to define against the variable background of normal density wood.

Some overlap could also be observed between the grey levels corresponding to knots and colored heartwood in the first two logs (Table 1), but this was deemed less relevant to defect scanning in maple, since knots and colored heartwood are both considered undesirable characteristics. Grey levels in the CT images could generally be used to separate sapwood from knots and from colored heartwood. Separating rot from sapwood was not so obvious but, given that rot in sugar maple logs normally occurs in the colored heartwood rather than sapwood, it should be possible to discriminate between the two by applying artificial intelligence. Generally speaking, if we consider the grey level scale in ascending order, from 0 to 256 (8 bits), the lower values represented rot while the higher ones denoted knots. Specifically, the grey level range 20–114 corresponded to rot; 87–136, to sapwood; 140–240, to colored heartwood; and 209–253, to knots (Table 1). In Group 2 as in Group 1, lower values corresponded to rot and higher values to knots.

Figures 4 and 5 show mean grey level values for individual wood types in the sample logs, and spread bars indicate corresponding standard
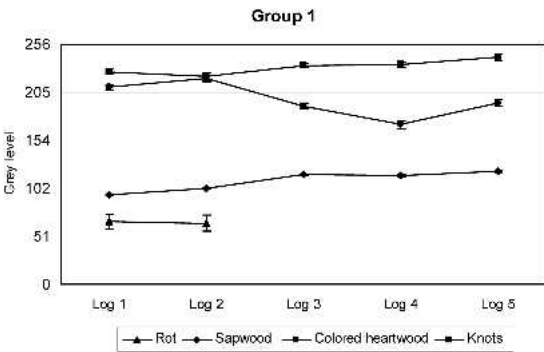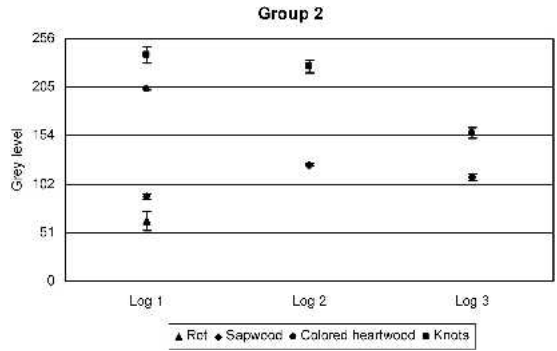

FIG. 5. Grey levels for individual wood types in logs without bark and undetermined cutting conditions and storage time.

errors for a specimen size of 1875 voxels. These figures indicate that sapwood can be separated from rot, colored heartwood, and knots if a sufficiently large number of pixels is considered for each type of wood. This information is of major importance since it suggests the feasibility of developing an automatic system for the detection of internal defects in sugar maple using X-ray technology.

Relationships between physical properties and CT image grey level

A correlation analysis was carried out to explore relationships between physical properties and grey levels in CT images. As shown in Table 4, strong correlations were found in all cases. Green density was the variable yielding the highest correlation with grey level, with a Pearson-correlation coefficient of more than 0.9 for all logs studied. This was expected because the level of attenuation of the X-ray signal is directly related to the mass of the scanned material. Consequently, a simple regression analysis was carried out between the green density and the CT image grey level (GL) for each type of wood. The grey level was used as the independent variable, and green density (GD) as the predicted variable in a model of the form $GD = B_o + B_1 GL$. The results of the regression analysis are shown in Table 5.

The relationships between green density and grey level for each type of wood (rot, sapwood,

FIG. 4. Grey levels for individual wood types in the various logs cut from a freshly-cut tree with bark.

TABLE 4. *Summary of Pearson-correlation coefficients between physical properties and grey levels for two log groups.*

| | Grey level | | | | | | | |
| | Group 1 | | | | | Group 2 | | |
Variables	Log 1	Log 2	Log 3	Log 4	Log 5	Log 1	Log 2	Log 3
Green density	0.94	0.95	0.96	0.92	0.96	0.96	0.92	0.93
Basic density	0.61	0.50	0.49	0.50	0.17	0.33	0.87	0.72
Moisture content	−0.17	0.26	0.64	0.49	0.63	0.48	0.74	0.76

TABLE 5. *Summary of parameters obtained from simple regression analysis for each type of wood in both log groups.*

| | Model Parameter | | | | |
Type of wood	b_0	b_1	S_{b1}	R^2	C.V.
Rot group 1	0.7083	0.0026	0.0002	0.76	7.0
Rot group 2	0.7066	0.0023	0.0003	0.80	6.3
Sapwood group 1	0.7809	0.0015	0.0001	0.38	2.8
Sapwood group 2	0.7616	0.0010	0.0001	0.51	4.4
Colored heartwood group 1	0.8321	0.0014	0.0001	0.72	2.3
Colored heartwood group 2	0.6800	0.0019	0.0001	0.82	3.9
Knots group 1	0.7958	0.0016	0.0002	0.46	2.1
Knots group 2	0.2279	0.0033	0.0009	0.32	8.2

C.V. = Coefficient of variation (%)
S_{b1} = Standard deviation of slope
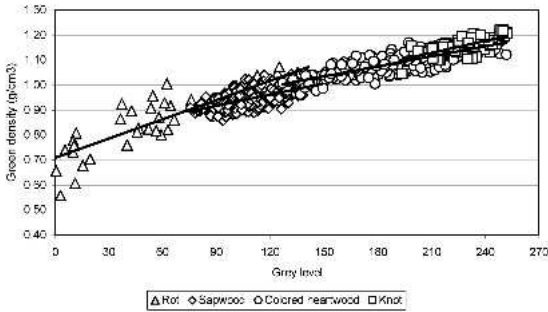R^2 = Coefficient of determination

FIG. 6. Scatter plot of relationship between grey level and green density for rot, knots, colored heartwood and sapwood in Group 1 logs.
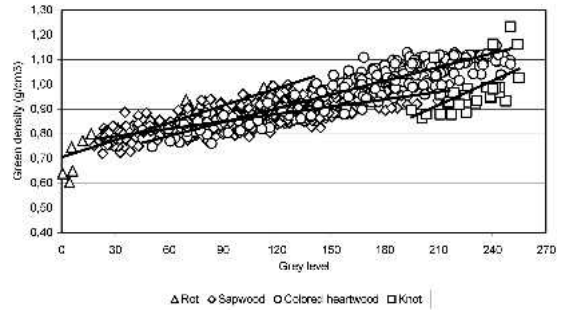

FIG. 7. Scatter plot of relationship between grey level and green density for rot, knots, colored heartwood and sapwood in Group 2 logs.

colored heartwood, and knot) from both groups of logs are shown in Figs. 6 and 7. Group 2 showed greater dispersion than Group 1. This dispersion can be attributed to the higher variability in green density for this group of logs, which can be associated with their different drying levels (log 2 was drier than logs 1 and 3), and by the fact that they came from different trees. In Fig. 6, a linear relationship can be observed between green density and grey level, with differences in the slope of the curve for each type of wood. Table 6 also shows that, for

both groups, the sapwood and colored heartwood tend to be characterized by lower slope values than rot and knots.

Comparisons between wood types in both groups revealed that rot and colored heartwood had respectively the least and greatest variation in slope values. This could indicate that different wood types give different responses to X-rays, suggesting that mass is not the only factor controlling the grey level to green density relationship. It is hypothesized at this stage that these differences might be attributed to the presence

and orientation of crystalline structures coming from the organized structure of cellulose in the woody cell wall. According to Bolt and Carrol (1963), the level of crystallinity plays a role in X-ray propagation in polymers. In medical science, Mostafavi et al. (1998) reported that stone composition (Urinary calculi) could be identified from the attenuation value obtained from a helical CT scanner. It remains, however, that the variability observed in attenuation values reflects the variability of crystalline components in different stones (Saw et al. 2000; Williams et al. 2001). In healthy, normally oriented wood, such as sapwood and heartwood, cellulose is organized mostly longitudinally in a crystalline structure. In knots, wood is also organized in a crystalline structure but in the transverse direction. Finally, rot is characterized by the relative deterioration of the crystalline cellulose ultra structures in the cell wall as a consequence of fungal wood degradation (Ohkoshi et al. 1999, Shimokawa et al. 2004).

In wood, the CT grey level response is determined by the bulk density of the material, but it was hypothesized, considering the literature on the matter, that it is also affected by the presence and orientation of crystalline structures mainly composed of cellulose in wood cell walls. Since the rot specimens showed different levels of degradation, an additional analysis was carried out with the goal of determining the effect of the degradation level on the response level to the radiation. The rot specimens were sorted into two groups according to the amount of rot present. In the first group, degradation affected more than 50% of the volume of the specimens. The second group consisted of the remaining specimens. Regression analyses of green density and CT image grey level carried out for both groups, and slopes in the resulting regression models were compared. As expected, the group with more rot exhibited a higher slope value (group A: $b_1 = 0.0063$, $S_{b1} = 0.0021$; group B: $b_1 = 0.0017$, $S_{b1} = 0.0002$). This result supports the hypothesis that the crystallinity level of the material also has an effect on material response to X-ray radiation. Additional work should be performed to further verify this hypothesis through a well designed and controlled experience.

CONCLUSIONS

The study of physical variables conducted in this research indicated that, in both groups of logs under test, wood type was the most significant source of variation in green density, basic density, and moisture content. Knots had the highest green density, followed by colored heartwood, sapwood, and rot respectively. Within each log group, mean green density values for each wood type were statistically different. The same trend was generally observed in mean basic density values, except that colored heartwood and sapwood showed somewhat similar values. The statistical analysis indicated that basic density was significantly different among wood types in Group 1. For Group 2, significant differences also existed between sapwood and the other wood types; the only exception was the difference between colored heartwood and sapwood, which was not significant.

The present study determined that grey level variations observed in CT images can serve as a basis to separate sapwood from colored heartwood and knots. The contrast in grey level between sapwood and rot areas was not so obvious even though rot was present only in the colored heartwood region. It consequently proved possible to distinguish sapwood from the other types of wood by applying a statistical approach with clusters of pixels. These results show real potential for the use of CT scanning to detect internal defects in sugar maple as a basis for sawing optimization.

Correlation analyses carried out for individual logs indicated that grey level variations in CT images were closely related to green density variations in corresponding to each of the log's internal characteristics. The regression analysis indicated the existence of a linear relationship between GL and green density, though with different slope values for the response curve of each wood type. It was hypothesized that part of the differences in response of each type of wood to X-ray radiation, in addition to density, can be attributed to the difference in the presence and

orientation of the crystalline structure in knots, colored heartwood, sapwood and rot. This hypothesis ought to be further confirmed in future studies.

Finally, moisture content variations associated with seasonal felling conditions and storage time should be further analyzed to cover overall moisture content variations at the sawmill headrig in relationship to the capacity of a CT scanner to detect internal defects in sugar maple logs. Future studies should be devised to better document the relationship between the CT image response and the various internal defect characteristics of sugar maple. With a better understanding of the causes of variation, it will be possible to envisage the development of specific software for the detection of internal defects in sugar maple logs as the first step in the creation of a sawing optimization package.

REFERENCES

ARCVIEW 3.2 user guide. 1999. Environmental Systems Research Institute. Inc. (ESRI). Redlands, CA.

BHANDARKAR, S. M., T. D. FAUST, AND M. TANG. 1999. CATALOG: A system for detection and rendering of internal log defects using computer tomography. Machine Vision and Application 1999(3):171–190.

BIRKELAND, R., AND W. HAN. 1991. Ultrasonic scanning for internal log defects. 4th International Conference on Scanning Technology in the Wood Industry. October 28–29, 1991, Burlingame, CA.

BJÖRKLUND, L. 1997. The interior knot structure of *Pinus sylvestris* stems. Scand. J. For. Res. 12:403–412.

———, AND H. PETERSSON. 1999. Predicting knot diameter of *Pinus sylvestris* in Sweden. Scand. J. For. Res. 14: 376–412.

BOLT, R. O., AND J. G. CARROLL. 1963. Radiation effects on organic materials. Academic Press. New York and London. 576 pp.

CHANG, S. J., J. R. OLSON, AND P. C. WANG. 1989. NMR imaging of internal features in wood. Forest Prod. J. 39(6):43–49.

CLARK, J., AND R. D. GIBBS. 1957. Studies in tree physiology. IV. Further investigations of seasonal changes in moisture content of certain Canadian forest tress. Can. J. Botany 35:219–253.

FUNT, B. V., AND E. C. BRYANT. 1987. Detection of internal log defects by automatic interpretation of computer tomography images. Forest Prod. J. 37(1):56–62.

GOOD, H. M., P. M. MURRAY, AND H. M. DALE. 1955. Studies on heartwood formation and staining in sugar maple, *Acer saccharum* Marsh. Can. J. Botany 33:31–41.

GUDDANTI, S., AND S. J. CHANG. 1998. Replicating sawmill sawing with TOPSAW using CT images of a full-length hardwood log. Forest Prod. J. 48(1):72–75.

HAGMAN, P. O. G., AND S. A. GRUNBDERG 1995. Classification of Scots pine (*Pinus sylvestris*) knots in density images from CT scanned logs. Holz Roh-Werkst. 53:75–81.

JENSEN, J. R. 1996. Introductory digital image processing: a remote sensing perspective. Prentice Hall, Upper Saddle River, NJ. 318 pp.

LAMB, F. M., AND R. M. MARDEN. 1968. Specific gravities Minnesota tree species. Forest Prod. J. 18(9):76–82.

———, AND ———. 1970. Variation in density of sugar maple sapwood and heartwood. USDA Forest Serv. Res. Note NC-90, 2 pp. N. Cent. Forest Exp. Sta., St. Paul, MN.

MOBERG, L. 2000. Models of internal knot diameter for *Pinus sylvestris*. Scand. J. For. Res. 15:177–187.

MOSTAFAVI, M. R., R. D. ERNST, AND B. SALTZMAN. 1998. Accurate determination of chemical composition of urinary calculi by spiral computerized tomography. J. Urol. 159(3):673–675.

NORDMARK, U. 2002. Knot identification from CT images of young *Pinus sylvestris* saw logs using artificial neural networks. Scand. J. For. Res. 17:72–78

OHKOSHI, M., A. KATO, K. SUZUKI, N. HAYASHI, AND M. ISHIHARA. 1999. Characterization of acetylated wood decayed by brown-rot and white-rot fungi. J. Wood Sci. 45:69–75.

OJA, J. 2000. Evaluation of knot parameters measured automatically in CT-images of Norway spruce (*Picea abies* (L.) Karst.). Holz Roh-Werkst. 58:375–379.

———, AND E. TEMNERUD. 1999. The appearance of resin pockets in CT-images of Norway spruce (*Picea abies* (L.) Karst.). Holz Roh-Werkst. 57:400–406.

PANSHIN, A. J., AND C. DE ZEEUW. 1980. Textbook of wood technology. McGraw-Hill, New York, NY. 722 pp.

PCI User Guide. 1997. Volume I. Version 6.1. Richmond Hill, ON, Canada.

PLATTEN D. 2002. http://www.impactscan.org/slides/impactday/basicct/sld001.htm

SAS INSTITUTE. 1988. Sas/Stat Users Guide, Release 6.03 Ed. Sas Institute, Inc., Cary, NC.

SAW, K C, J. A. MCATEER, A. G. MONGA, G. T. CHUA, J. E. LINGEMAN, AND J. C. WILLIAMS, Jr. 2000. Helical CT of urinary calculi: Effect of stone composition, stone size, and scan collimation. AJR Am. J. Roentgenol. 175:329–332.

SEERAM, E. 2001. Computed tomography: physical principles, clinical applications, and quality control. 2nd ed. W.B. Saunders Company, Philadelphia, PA. ISBN 0–7216–8173–5. 430 pp.

SHIMOKAWA, T., M. NAKAMURA, N. HAYASHI, AND M. ISHIHARA. 2004. Production of 2,5-dimethoxyquinone by the brown-rot fungus *Serpula lacrymans* to drive extracellular Fenton reaction. Holzforschung 58:305–310.

SIMPSON W., AND A. TENWOLDE. 1999. Physical properties and moisture relations of wood. Wood Handbook: Wood as an Engineering Material. Forest Product Society.

SOM, S., I. SVALBE, J. DAVIS, J. GRANT, E. GOLD, K. TSUI, AND P. WELLS. 1995. Internal scanning of logs for grade evaluation and defect location. Proc. DICTA-95 Digital Image Computing: Technologies and Applications. December 1995, Brisbane, Australia.

STEELE, P. H., M. W. WADES, S. H. BULLARD, AND P. A. ARAMAN. 1992. Relative kerf and sawing variation values for some hardwood sawing machines. Forest Prod. J. 42(2):33–39.

———, T. E. G. HARLEES, F. G. WAGNER, L. KUMAR, AND F. W. TAYLOR. 1994. Increased lumber value from optimum orientation of internal defects with respect to sawing pattern in hardwood sawlogs. Forest Prod. J. 44(3):69–72.

TAYLOR, F. W., F. G. WAGNER, JR., AND C. W. MCMILLIN. 1984. Locating knots by industrial tomography-A feasibility study. Forest Prod. J. 34(5):42–46.

WAGNER, F. G., F. W. TAYLOR, D. S. LADD, C. W. MCMILLIN, AND F. L. RODER. 1989. Ultrafast CT scanning of an oak log for internal defects. Forest Prod. J. 39(11/12):62–64.

WILLIAMS, JR, J. C., K. C. SAW, A. G. MONGA, G. T. CHUA, J. E. LINGEMAN, AND J. A. MCATEER. 2001. Correction of helical CT attenuation values with wide beam collimation: in vitro test with urinary calculi. Acad. Radiol. 8(6):476–483.

ZHU, D., R. W. CONNERS, F. LAMB, AND P. A. ARAMAN. 1991. A computer vision system for locating and identifying internal log defects using CT imagery. Pages 1–13 *in* Proc. Fourth International Conference on Scanning Technology in the Wood Industry, Burlingame, CA.